J Cancer Res Clin Oncol (2011) 137:1349–1361
DOI 10.1007/s00432-011-1005-1

ORIGINAL PAPER

RP101 (brivudine) binds to heat shock protein HSP27 (HSPB1) and enhances survival in animals and pancreatic cancer patients

Jörg-Christian Heinrich · Anne Tuukkanen · Michael Schroeder · Torsten Fahrig · Rudolf Fahrig

Received: 6 May 2011 / Accepted: 4 July 2011 / Published online: 22 July 2011

Abstract
Background Several reports describe the importance of the chaperone HSP27 (HSPB1) in cancer progression, and the demand for drugs that modulate HSPB1-activity is increasing rapidly. We reported earlier that RP101 (Bromovinyldeoxyuridine, BVDU, Brivudine) improves the efficacy of chemotherapy in pancreatic cancer.
Methods *Chemistry*: Binding of RP101 and HSPB1 was discovered by affinity chromatography. *Molecular and cell biology*: HSPB1 in vitro transcription/translation (TNT), Pull down using RP101-coupled magnetic beads, Immuno Co-precipitations, Structural modeling of HSP27 (HSPB1), Introduction of point mutations into linear expression templates by PCR, Heat shock, Tumor Invasion. *Animal experiments:* Treatment of AH13r Sarcomas in SD-rats. *Clinical Studies with late-stage pancreatic cancer patients:* Pilot study, Dose finding study, Phase II study (NCT00550004).
Results Here, we report that RP101 binds in vitro to the heat shock protein HSPB1 and inhibits interaction with its binding partners. As a result, more activated CASP9 was detected in RP101-treated cancer cells. We modeled HSPB1-structure and identified the RP101 binding site. When we tested RP101 as an anti-cancer drug in a rat model, we found that it improved chemotherapy. In clinical studies with late-stage pancreatic cancer patients, the dose of 500 mg/day was safe and efficient, but 760 mg/day turned out to be too high for lightweight patients.
Conclusions The development of RP101 as a cancer drug represents a truly novel approach for prevention of chemoresistance and enhancement of chemosensitivity.

Keywords HSP27 (HSPB1) · Chemotherapy · Chemoresistance · Molecular chaperones · Pancreatic cancer

Introduction

Pancreatic ductal adenocarcinoma is the 4–5th most common cancer in the western world. Its mortality almost equals its incidence rate of 6.3/100,000 (Jemal et al. 2007). Resection of the tumor, the only treatment with curative intent, is only possible in about 10–20% of patients because of the late clinical manifestation and the unfavorable location of the malignancy (Alexakis et al. 2004). Although more than 30 anti-cancer drugs have been described, the results of treatment with these alone or in combination with radiation or another cytotoxic drug are unsatisfactory. The failure of chemotherapeutic strategies is largely due to the chemoresistance of the tumor cells (Murr et al. 1994; Wolff et al. 2000; Neoptolemos et al. 2004).

HSPB1 (heat shock 27 kDa protein 1, HSP27) is involved in a number of processes such as apoptosis, DNA repair, and recombination. It regulates apoptosis through interaction with STAT3 (Song et al. 2004; Hsieh et al. 2005; Rocchi et al. 2005; Lee et al. 2008), CYC1 (Cytochrome c-1) (Pandey et al. 2000), and CASP3 (Caspase 3) (Rocchi et al. 2006; Batchelder et al. 2009). It has been suggested that the anti-apoptotic effect of HSPB1 overexpression is associated with altered DNA topoisomerase II

J.-C. Heinrich · T. Fahrig · R. Fahrig (✉)
RESprotect, Fiedlerstr. 34, 01307 Dresden, Germany
e-mail: fahrig@resprotect.de

A. Tuukkanen · M. Schroeder
Biotec/Department of Computing,
Technical University Dresden, Dresden, Germany

expression (Hansen et al. 1999). Low levels of expression are associated with resistance (Harris and Hochhauser 1992). Topoisomerase II is known as a target for chemotherapy (Nitiss 2009). DNA topoisomerases are involved in several aspects of DNA metabolism, in particular in genetic recombination. This is consistent with the observation that HSPB1 plays a role in DNA repair and base excision (Nadin et al. 2003; Mendez et al. 2000). Additionally, HSPB1 protects cells from monocyte cytotoxicity (Mahvi et al. 1993; Jaattela and Wissing 1993).

The role of heat shock protein HSPB1 in reducing resistance to chemotherapy of pancreas and other cancers has been recently described (Chauhan et al. 2003; Mori-Iwamoto et al. 2007). Increased HSPB1 expression is related to higher rates of Gemcitabine (GEM) resistance in patients with pancreatic cancer. Furthermore, knock-out of HSPB1 reduces chemoresistance (Mori-Iwamoto et al. 2007). Importantly, HSPB1 is up-regulated across many types of cancer, including prostate (Song et al. 2004), colorectal (Zhao et al. 2007), liver (Feng et al. 2005), breast (Kang et al. 2008), skin (Wang et al. 2009), bladder (Kamada et al. 2007; Rane et al. 2003), eye (Kase et al. 2009), ovarian (Xia et al. 2009), and pancreas (Xia et al. 2009). In some of these cancers, such as ovarian, liver, bladder, and eye, HSPB1 is also implicated in chemoresistance (Nitiss 2009).

In summary, HSPB1 regulates apoptosis and is linked to chemoresistance in numerous cancers. Thus, modulating the activity of HSPB1 is a promising approach to tackle chemoresistance in cancer (Xia et al. 2009). In the present study, we describe the first small molecule, RP101 that binds to HSPB1, and show that this binding disrupts the interaction of HSPB1 and downstream effectors such as CASP3, CYC1, and AKT1. We developed an in silico 3D model of the structure of HSPB1 and identified a potential binding site for RP101. We confirmed this binding site by mutating two key residues in the active site**.** Besides unraveling in vitro the molecular mechanism by which RP101 modulates HSPB1, we confirmed the hypothesis that RP101 is a potent drug against chemoresistance with experimental evidence in animal models and three clinical studies with late-stage pancreatic cancer patients.

Materials and methods

Chemicals

Gemcitabine (GEM) was purchased from Eli Lilly, and RP101 ((E)-5-(2-Bromovinyl)-2′-Deoxyuridine) was by RESprotect. All of the other chemicals were from Sigma–Aldrich (Taufkirchen, Germany) and Roth (Karlsruhe, Germany) unless otherwise indicated.

Molecular and cell biology

Unless otherwise indicated, all molecular procedures were performed as described (Fahrig et al. 2003; Fahrig et al. 2006).

Cell lines

BxPC-3 cells (human pancreatic adenocarcinoma) were obtained from ATCC (http://www.lgcstandards-atcc.org). Cells were grown in RPMI 1640 medium supplemented with 10% fetal bovine serum, penicillin, streptomycin, and 1 mM sodium pyruvate.

HT1080 cells (human fibrosarcoma) were purchased from DSMZ GmbH, Braunschweig, Germany. Cells were treated with Gemcitabine (10 ng/ml) with and without RP101 (30 μM). After trypsinisation, the number of living cells was determined using the Cell Counter and Analyzer System CASY TT (Schärfe System GmbH, Reutlingen, Germany). Granta-519 cells (human B cell lymphoma) were purchased from DSMZ GmbH, Braunschweig, Germany. Logarithmically growing cells were seeded at a density of 100,000 cells/ml and incubated for 24 h with 15 ng/ml Gemcitabine. Cultures for Western Blotting were treated with or without RP101 (15 and 30 μM). AH13r cells, a subline of the rat Yoshida sarcoma, were obtained from the Cell and Tumor Bank of the West German Cancer Center, University Essen, Medical School (Essen, Germany). Cells were treated with 35 ng/ml Mitomycin C(MMC) with or without RP101 (30 μM).

HSPB1 in vitro transcription/translation (TNT)

HSPB1 protein was synthesized in vitro using a PCR expression template.

HSPB1 full length cDNA and the following primers were used for PCR. PCR-Primer Forward (containing T7 primer-sequence): 5′-TAC ATC TAC TTA ATA CGA CTC ACT ATA GGG GCC AGC ATG ACC GAG CGC CGC GT-3′. PCR-Primer Reverse (containing HIS-tag and poly A tail): 5′-TTT TTT TTTTTTTTT AGT GGT GAT GGT GAT GAT GCT TGG CGG CAG TCT CA-3′. PCR products were cleaned up using the Qiagen PCR purification kit. Purified PCR expression templates were then used for in vitro Transcription/Translation (Promega kit TNT T7 Quick for PCR DNA) to produce HSPB1 protein or HIS-tagged HSPB1 protein. Approximately 400 ng of HSPB1 protein was used for each pull-down experiment.

Pull down using RP101-coupled magnetic beads

HSPB1 protein was incubated with RP101-coupled magnetic beads in the appropriate binding buffer. In parallel,

HSPB1 was incubated with control beads. Proteins were washed, eluted, concentrated using the method described by Wessel and Flügge (1984), separated by denaturing PAGE, and transferred to a PVDF membrane by Western Blotting. Samples were probed for HSPB1 protein (HSP27 antibody, Santa Cruz: sc-1048). Images were acquired using the Kodak Image Station 440 and the Kodak 1D Image Analysis Software, Version 3.5.

Immuno co-precipitations

HIS-tagged HSPB1 protein was synthesized in vitro and coupled to magnetic HIS-Tag Isolation and Pulldown beads (Dynabeads, Invitrogen) according to manufacturer's instructions. Granta-519 cells were incubated for 24 h with 15 ng/ml Gemcitabine. RP101 (300 µM or 3 mM) was added to the protein lysate after homogenization. HIS-tagged HSPB1 protein was incubated with approximately 2 mg of Gemcitabine-treated total protein in a volume of 500 µl. HSPB1 bound proteins were pulled down magnetically, washed four times, eluted in HIS elution buffer, concentrated using the method described by Wessel and Flugge (1984), separated by denaturing PAGE, and transferred to a PVDF membrane by Western Blotting. Samples were probed for HSPB1 (HSP27 antibody, Santa Cruz: sc-1048), Pro-CASP3 (CASP3 antibody, BD Transduction Laboratories: 610322), AKT1 (AKT antibody, Cell Signaling: 9272), or CYC1 protein (Cytochrome C antibody, BD Pharmingen: 556433).

Structural modeling of HSP27 (HSPB1)

A three-dimensional structural model of HSPB1 was produced using SAM-T08 web server (Karplus 2009) following the procedure in Fig. 2. The three-dimensional structure of a small metazoan heat shock protein TSP36 was used as a modeling template (PDB identifier 2bol). The overall sequence identity with the used template protein structure was 23%. The C-terminal part of HSPB1 contains an approximately 90-residue long "alpha-crystallin domain," typical of small heat shock proteins, for which the sequence identity is higher.

The modeled structure was subjected to conjugate gradient minimization using the program NAMD2 (Phillips et al. 2005) and the CHARMM27 force-field. The TIP3P solvent model represented the water molecules. Simulations assumed constant particle number, constant pressure, and constant temperature (NpT) ensembles. Langevin dynamics were used to maintain constant temperature, and pressure was controlled using a hybrid Nose–Hoover Langevin piston method. Extensive molecular dynamics simulations were done on the modeled structure in order to study its quality and structural stability.

Binding sites were predicted on the model structure with the help of LIGSITEcsc server (Huang and Schroeder 2006), which identifies the three largest and best conserved pockets on the protein surface. These pockets were studied manually and compared to the physico-chemical features of a known RP101 binding site in a viral thymidine kinase (Protein Databank IDs 1KI8, 1OSN, 2W0S). The RP101 binding site on the viral thymidine kinase has two aromatic residues (analogous to Phe29 and Phe33 in HSPB1) forming a stacking effect with favorable van der Waals interactions with the ring structure of RP101.

Introduction of point mutations into linear expression templates by PCR

The basic procedure that was adapted for the introduction of point mutations is called "two-sided splicing by overlap extension" (Horton et al. 1989). Starting from the HSPB1 wildtype PCR template described above, two separate PCRs were used to generate two primary PCR products a and b. Both primary PCR products contained the desired mutation within overlapping regions. These overlaps were needed for the production of the full length expression template (PCR c) containing the appropriate mutation. Point mutations were confirmed by sequencing.

Heat shock

Since one of the known functions of HSPB1 is the protection of the cell against elevated temperatures, we tested if heat shock caused more severe effects on cultured cells in the presence of RP101. Cells were treated with 35 ng/ml Mitomycin C(MMC) with or without RP101 (30 µM).

Tumor invasion

The influence of RP101 on the invasiveness of the fibrosarcoma cell line HT-1080 was tested using the "BD BioCoat Tumor Invasion System." Cells were incubated for 3 days with Gemcitabine ± RP101 and then seeded on 24-well matrigel culturing plates. After 20–22 h, cells that penetrated the matrigel were stained with Calcein AM and quantified using a TecanGenios plate reader.

Treatment of AH13r sarcomas in SD-rats

Ten SD-rats per treatment group received a single injection of ascites Yoshida AH13r hepatoma cells subcutaneously. Five to 7 days after tumor application, the growth of the tumors was suppressed by i.p. treatment of the animals with 2 or 4 mg/kg doxorubicin (9 times within 3 weeks), 120 or 140 mg/kg glufosfamide (15 times within 3 weeks), and 0.5 or 1.5 mg/kg cisplatin only (4 or 5 times within 3 weeks),

and by additional oral treatment with 15 mg/kg RP101 (15 times within 3 weeks).

Based on our previous results with rats, a daily dose of 15 mg/kg RP101 was used (Fahrig et al. 2003) for co-treatment. RP101 was administered as shown in Fig. 4.

Clinical studies

Pilot study

The study was conducted with four stage III, and 9 stage IV pancreatic cancer patients. Patients were treated i.v. with 1,000 mg/m^2 GEM, 50 mg/m^2 cisplatin and RP101 (4 × 125 mg tablets per day) (Fahrig et al. 2006) as shown in Fig. 5a.

Dose finding study

To evaluate a dose range of RP101 with a fixed dose of Gemcitabine (1,000 mg/m^2) (Fahrig et al. 2006), twenty-two patients with advanced pancreatic adenocarcinoma were eligible for treatment in this single arm study. The mean age was 60 years and 73% of patients were men. One patient without progressive disease was excluded from the study for withdrawal of consent after the first cycle. Of the 21 patients left, 15 were in stage IV and 6 in stage III. RP101 was administered in combination with GEM as shown in Fig. 5b. The starting dose of RP101 was 4 × 125 mg/day (total dose of 6,000 mg per treatment cycle) together with a fixed dose of GEM (1,000 mg/m^2). Subsequently, using 125 mg tablets, total doses of RP101 per cycle were 7,500, 9,000, 10,500, and 12,000 mg in four patients per dose (Fahrig et al. 2006).

Phase II study (NCT00550004)

A randomized, placebo-controlled, double-blind clinical trial conducted with 168 patients of stage III (25%) and IV (75%) at 50 sites throughout the United States, Europe, and South America was performed. The mean age was 61 years and 61% of patients were men. The MITT (modified intent to treat) population was 151 patients. Two thirds of the patients assigned to the treatment arm received 4 × 190 mg RP101 tablets/day in combination with GEM (1,000 mg/m^2) as shown in Fig. 5c, while one third of the patients in the control arm received GEM plus placebo.

The study was performed by SciClone Pharmaceuticals/USA using the dose selected in the dose finding study by Avantogen Oncology/USA, whereas the analysis of the patient data was done by RESprotect/Germany. The ethical committees of all performing institutions and the specific approval authorities of the different countries have approved the clinical studies. We confirm that the informed consent was obtained from all patients.

Statistics

Cox Regression Analysis was carried out using factor treatment, factor body surface area (BSA), and Kaplan–Meier Survival analysis with log-rank tests. Analyses were performed via SAS 9.2, validation via SPSS 15. The study evaluated a mix of both stage III and stage IV patients.

Results

Molecular and cell biology

Binding of RP101 and HSPB1

Binding of RP101 and HSPB1 was discovered by affinity chromatography. We used magnetic beads coupled to RP101 and empty beads as controls to pull out proteins from cell lysates (BxPC-3 cells). The one predominant binding partner identified by mass spectroscophy (nanoLC-ES-MSMS) was HSPB1. To find out whether the interaction between RP101 and HSPB1 was direct or indirect, we synthesized HSPB1 in vitro.

Direct interaction of in vitro synthesized HSPB1 protein with RP101

To test if RP101 interacts with HSPB1 directly, we carried out pull-down experiments with magnetic beads coupled to RP101 and empty beads as controls followed by Western Blot. In vitro synthesized HSPB1 protein was incubated with RP101 coupled to magnetic beads. Figure 1a shows that HSPB1 was pulled down by RP101, whereas the empty beads did not bind.

Structural model of human heat shock protein HSPB1 and RP101 binding site

To visualize the interaction between RP101 and HSPB1, we developed a three-dimensional structural model of HSPB1 and the predicted binding site of RP101 (Fig. 2a). The model was generated in four steps (see Fig. 2b–e). First, we used the structure prediction program SAM-T08, which generates good quality structures across all classes of predictions as evaluated in the CASP8 structure prediction assessment (Phillips et al. 2005). Second, we ran extensive molecular dynamics simulations, which confirmed the model's quality and structural stability with only average fluctuations across the model of 1.7 Å. Third, we predicted possible binding sites. Generally, binding sites are characterized by pockets with conserved residues, which are important for function. Using the program LIGSITEcsc (Huang and Schroeder 2006), we identified the three

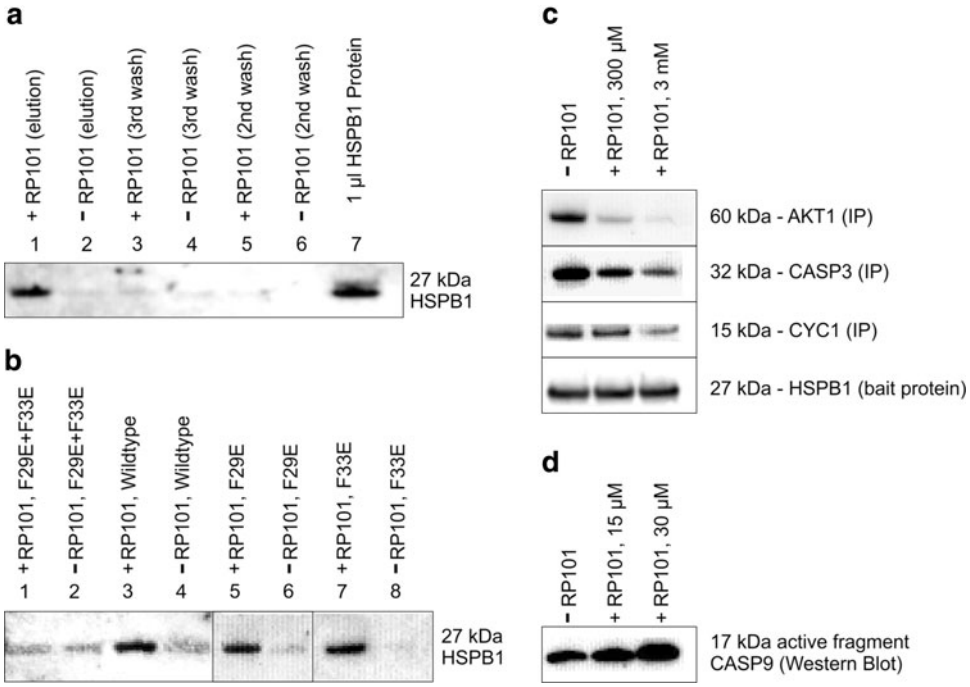

Fig. 1 RP101 binds directly to HSPB1 and inhibits interaction with binding partners. **a** In vitro synthesized HSPB1 protein is pulled down by magnetic beads coupled to RP101 (*lane 1*) but not by control beads missing RP101 (*lane 2*). Pull-down experiment with wildtype HSPB1 protein and RP101-magnetic beads followed by Western Blot. *Lane 7* shows in vitro synthesized HSPB1 protein before incubation with magnetic beads and subsequent washing steps. **b** Double mutation Phe29Glu plus Phe33Glu destroys RP101 binding site. HSPB1 with double mutation Phe29Glu (F29E) plus Phe33Glu (F33E) does not bind to RP101 magnetic beads (*lane 1*), whereas the single mutations and wildtype bind. Pull-down experiment with HSPB1 wildtype protein synthesized in vitro, HSPB1 mutations and RP101-magnetic beads followed by Western Blot. Membranes have been cut to show relevant bands. **c** RP101 binding to HSPB1 inhibits interaction with binding partners. Less AKT1 protein, Pro-CASP3, and CYC1 (Cytochrome C) co-precipitate with HIS-tagged HSPB1 in the presence of RP101 from protein lysate. Immunoprecipitations followed by Western Blot. Granta-519 cells pretreated with 15 ng/ml Gemcitabine for 24 h. Identical amounts of HIS-tagged HSPB1—the bait-protein—are detected in all lanes independent of the treatment. *Lane 1* without RP101, *lane 2* 300 µM RP101, *lane 3* 3 mM RP101. **d** RP101 binding to HSPB1 induces CASP9 activation. More activated CASP9 is detected by Western Blot in Granta-519 cells treated 24 h with 15 ng/ml Gemcitabine and RP101. *Lane 1* Gemcitabine—without RP101, *lane 2* Gemcitabine + 15 µM RP101, *lane 3* Gemcitabine + 30 µM RP101

deepest pockets with best conservation of residues. Fourth, the three binding sites were studied manually and compared to the physico-chemical features of a known RP101 binding site in a viral thymidine kinase (UL23) (Champness et al. 1998; Bird et al. 2003; Caillat et al. 2008) (PDB identifiers: 1KI8, 1OSN, 2W0S). The RP101 binding site on the kinase has two aromatic residues forming a stacking effect with favorable van der Waals interactions with the ring structure of RP101 (see Fig. 2). In the modeled structure, a similar binding site was identified with two phenylalanine residues (Phe29 and Phe33). These residues are only moderately conserved in heat shock proteins, possibly since RP101 is not a natural ligand for this protein.

Proof of HSPB1–RP101 binding site through double mutant Phe29Glu, Phe33Glu

We examined the HSPB1 model created in silico by exchanging the amino acids at the predicted binding sites. In vitro synthesized HSPB1 was incubated with RP101 coupled to magnetic beads and in parallel with control beads without RP101. Point mutations were introduced at position Phe 29 and Phe 33 of the wildtype HSPB1 protein to study the effects on the RP101 binding site as predicted by the in silico model. Figure 1b presents the results from pull-down experiments with HSPB1 mutants. Phenylalanine residues were exchanged to glutamic acid first individually and then both simultaneously in a double mutant. The Phe29Glu mutation did not have any effect on the RP101 binding. The same was true for the single Phe33Glu mutation. However, the mutation of both Phe29 and Phe33 to glutamic acids prevented RP101 binding. Point mutations were introduced also at positions Phe19, Trp22, and Trp45 of HSPB1 protein to check other possible RP101 binding sites as predicted by the in silico model. Phe19, Trp22, and Trp45 were exchanged with glutamic acid. HSPB1 with the mutation Trp22Glu, Trp45Glu, and the double mutation Phe19Glu and Trp22Glu still interacted with RP101-beads like the wildtype HSPB1 protein (data not shown).

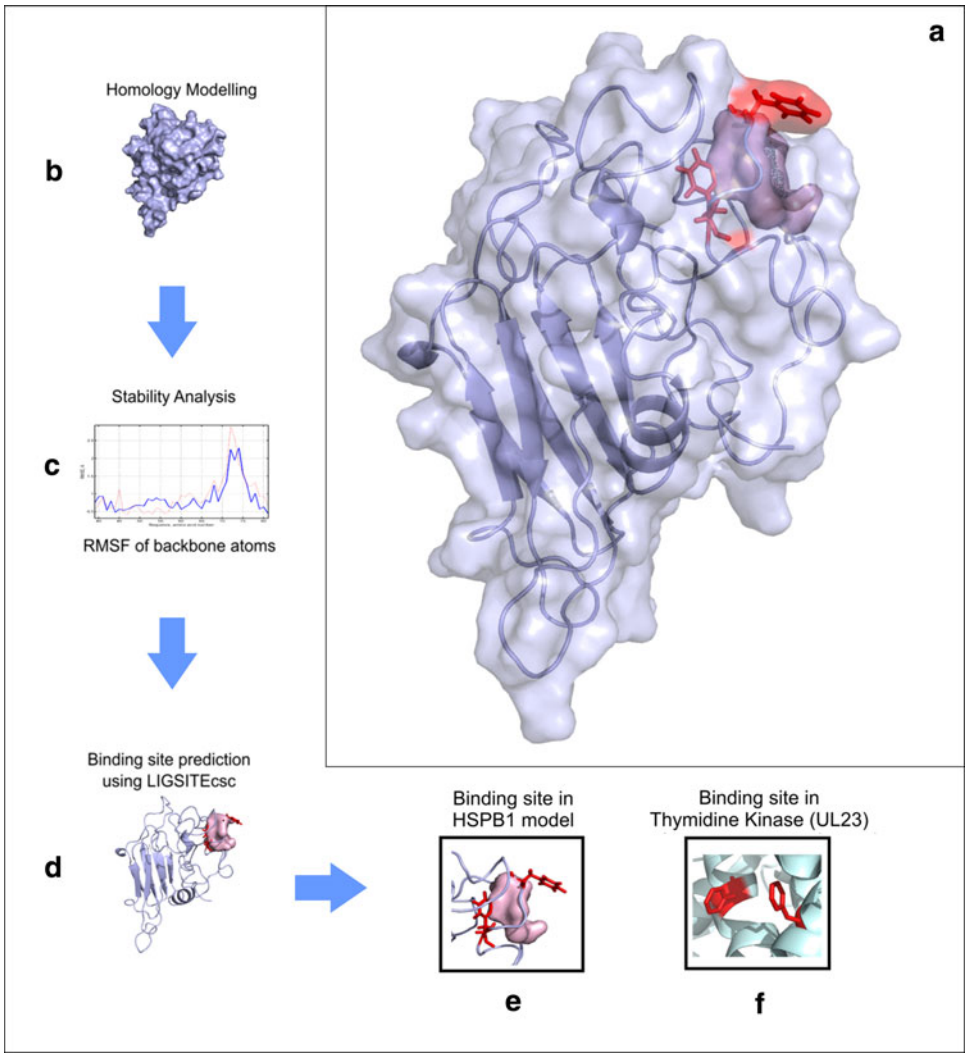

Fig. 2 **a** Three-dimensional model of HSPB1 with the predicted RP101 binding site around Phe29 and Phe33. **b–e**, Workflow to obtain model and predicted binding site. **b** Raw homology model of HSPB1 based on metazoan heat shock protein at 23% sequence identity. **c** Comprehensive energy minimization with molecular dynamics simulation refines raw model. **d** Identification of large, conserved pockets on surface. **e** Predicted RP101 binding site on HSPB1 is one of the pockets with two phenylalanines in similar conformation as in the kinase. **f** Known RP101 binding site in viral thymidine kinase with two phenylalanines

RP101-mediated inhibition of HSPB1 interactions

HSPB1 regulates apoptosis through its interaction with Pro-CASP3 (Rocchi et al. 2006; Batchelder et al. 2009), AKT1 (Rane et al. 2003), and CYC1 (Pandey et al. 2000). According to Rane et al. (2003), disruption of the interaction between HSPB1 and AKT1 impairs AKT1 activation, leading to an enhanced rate of apoptosis. Thus, the question arises whether RP101 affects HSPB1's ability to bind these proteins. To answer this, we carried out immune precipitations followed by Western Blotting. Figure 1c shows that with RP101 binding to HSPB1, there was less AKT1 protein, Pro-CASP3, and CYC1 co-precipitated with HIS-tagged HSPB1. These findings confirmed the inhibitory effect of RP101 and its effect on apoptosis.

RP101 effect on CASP9 (caspase 9) activation

CASP9 activation as a result of HSPB1 inhibition has been described earlier and accordingly more activated CASP9 (Cleaved Caspase-9 antibody, Cell Signaling: 9501) was detected in RP101-treated Granta-519 cells by Western Blotting (Fig. 1d).

RP101 inhibited cell growth after heat shock

Cells were treated with 35 ng/ml Mitomycin C(MMC) with or without RP101 (30 μM). Without heat shock this dosage is tolerated by this cell line (Fahrig et al. 2003). As shown in Fig. 3, after 11 days of treatment, the cells started to grow rapidly in the MMC group. RP101 inhibited this growth.

Tumor invasion in vitro

In order to verify RP101's effect on metastases, we used the penetration of human HT-1080 fibrosarcoma cells through a matrigel matrix as a model for tumor invasion. The treatment of HT-1080 cells with Gemcitabine together with RP101 reduced penetration through matrigel by 30–50%

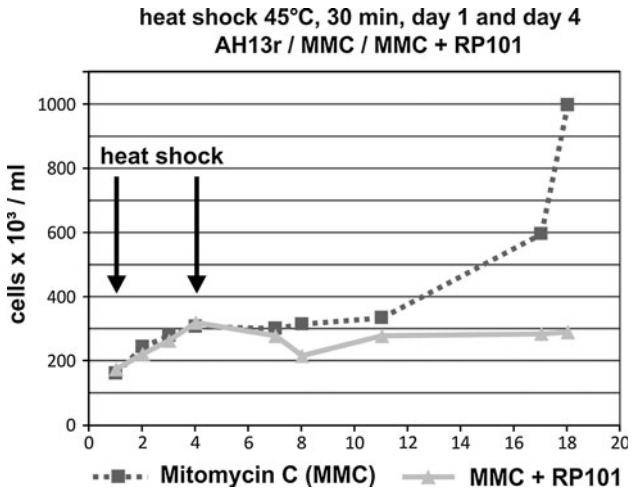

Fig. 3 RP101 inhibits cell growth after heat shock. AH13r cells treated with 35 ng/ml Mitomycin C(MMC) with or without RP101 (30 μM). After 1 and 4 days of treatment, cells were heat-shocked for 30 min at 45°C

compared to cells treated with Gemcitabine alone (data not shown).

Treatment of AH13r sarcomas in Sprague–Dawley (SD)-rats

SD-rats were treated with corn oil alone, RP101 alone or in combination with Cisplatin or cyclophosphamide (Fig. 4). Fig. 4a shows that RP101, when given alone, exerted no influence on the growths of rat tumors. Figure 4b shows that RP101, when given exclusively in parallel with Cisplatin, had only a weak effect. Figure 4c shows that RP101, when given together with Cisplatin and thereafter for 2–3 days alone in the "recovery" phase, had a strong effect. Figure 4d shows that RP101, when given only once at the beginning of treatment together with cyclophosphamide and thereafter 15 times alone in the "recovery" phase, had a very strong effect.

The result of chemotherapy without RP101 "recovery" treatment showed that the effect was only weak. In these experiments, the dose of RP101 was very high, i.e., 50 mg/kg. This was much more than the standard dose of 15 mg/kg. When RP101 was given afterwards for 2–3 days alone in the "recovery" phase, this treatment with even lower doses of Cisplatin was effective. A prolongation of the treatment in the "recovery" phase was shown with cyclophosphamide. Of the cytotoxic drugs tested, cyclophosphamide had the best long-term effects and gave an excellent example for the "recovery" phase effect. In summary, the experiments showed that in an animal model RP101 had no effect on its own, but strong effects in combination with chemotherapy.

Clinical studies: RP101 as co-treatment in late-stage pancreatic cancer patients

Mode of application

The clinical application of the above-mentioned results can be seen in the following studies with pancreatic cancer patients: *Pilot Study* (Fig. 5a) 2 × 4 days "recovery" treatment; *Dose Ranging Study* (Fig. 5b) 3 × 3 days "recovery" treatment; *Phase II Study* (Fig. 5c) 3 × 3 days "recovery" treatment.

Pilot study

The data from patients treated with RP101 were compared to data from historical controls. Median survival was 14.7 months in the RP101 group and 6.2 months in the historical control group (Fig. 5d) (Fahrig et al. 2006).

Dose finding study

The median survival for all 22 patients in this study with doses of 500, 625, 750, 875, and 1,000 mg/day (4–8 × 125 mg tablets/day) was 9.3 months in the RP101 group (Fig. 5e) and 5.6 months in the historical control group. The two highest doses (875 and 1,000 mg/day) showed side effects related to Gemcitabine. Side effects related to RP101 were not observed at any of the doses evaluated (Fahrig et al. 2006).

Based on the data from the dose finding study with each four patients per dose, a dose of 760 mg/day (4 × 190 mg/day) was selected for a phase II clinical trial. However, this dose turned out to be too high for lightweight patients.

Pharmacokinetic data of RP101

The first dose of RP101 was given half an hour prior to Gemcitabine administration and the second dose 4 h thereafter. At this time, Gemcitabine was below the limit of detection. The results are summarized in Table 1a.

Phase II study (NCT00550004)

Median survival was statistically higher in the GEM + placebo group than in the GEM + RP101 group. Drug overdosing was seen in patients with a body surface area (BSA). BSA $\leq 1.85\ m^2$ (BSA (m^2) was calculated according to the Dubois Formula: $0.20247 \times \text{Height}\ (m)^{0.725} \times \text{Weight}\ (kg)^{0.425}$). Half of the patients had a BSA $\leq 1.85\ m^2$, half a BSA $> 1.85\ m^2$. In patients with a BSA $\geq 1.85\ m^2$, there was no significant difference in median survival (trend threshold; Table 1b; Fig. 6). Patients starting at a BSA $> 1.85\ m^2$ showed benefit from the co-treatment with RP101. Only low or no drug overdosing effects have been detected with increasing BSA (Fig. 6).

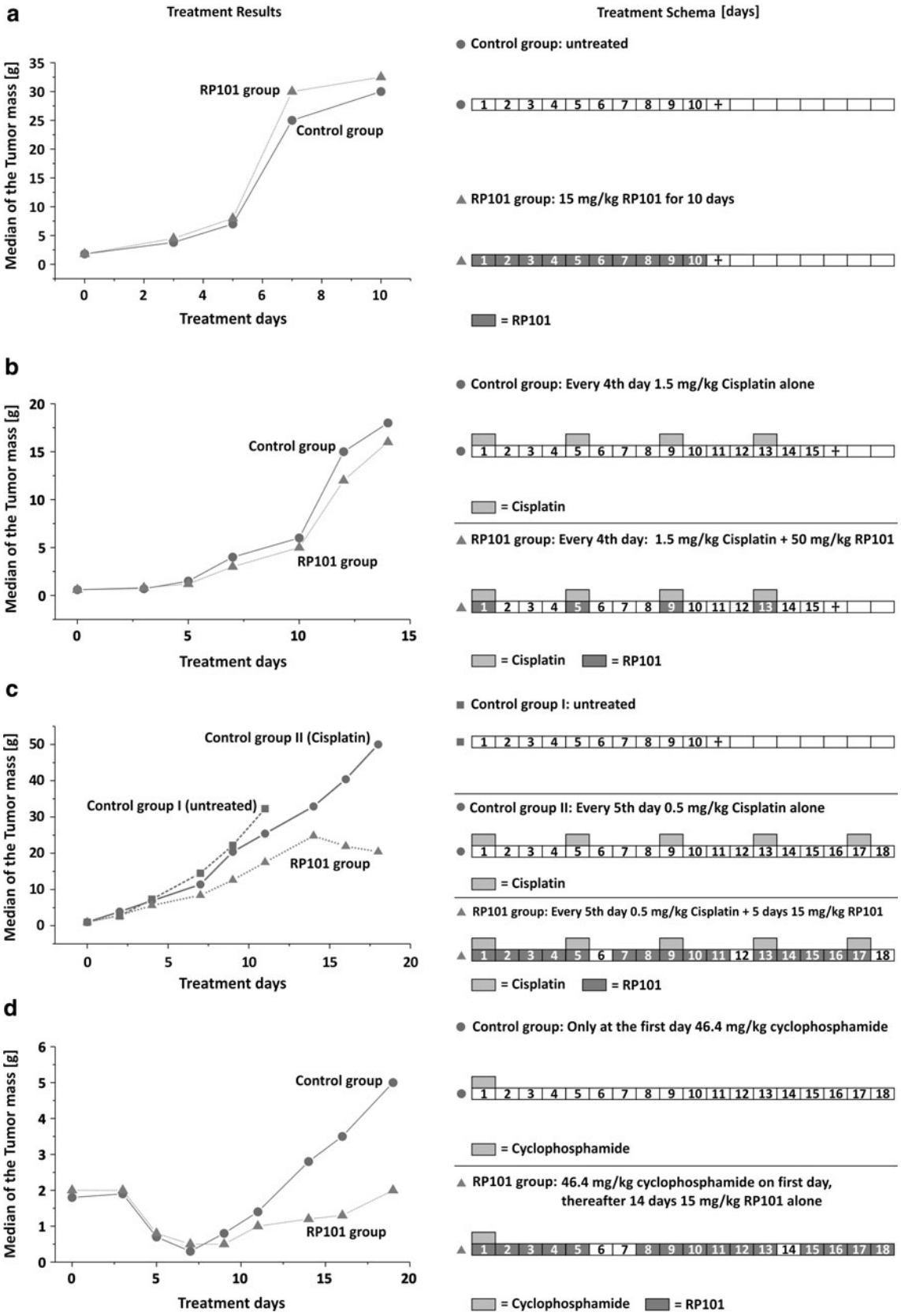

Fig. 4 RP101 with cisplatin or cyclophosphamide can significantly reduce the growth of AH13r Sarcomas in SD-rats. **a** RP101 alone does not influence tumor growth. **b** RP101 given with cisplatin simultaneously has a weak effect. **c** RP101 with cisplatin and additionally alone in "recovery"-phase has a strong effect. **d** RP101 with cyclophosphamide and alone in "recovery"-phase has a strong effect

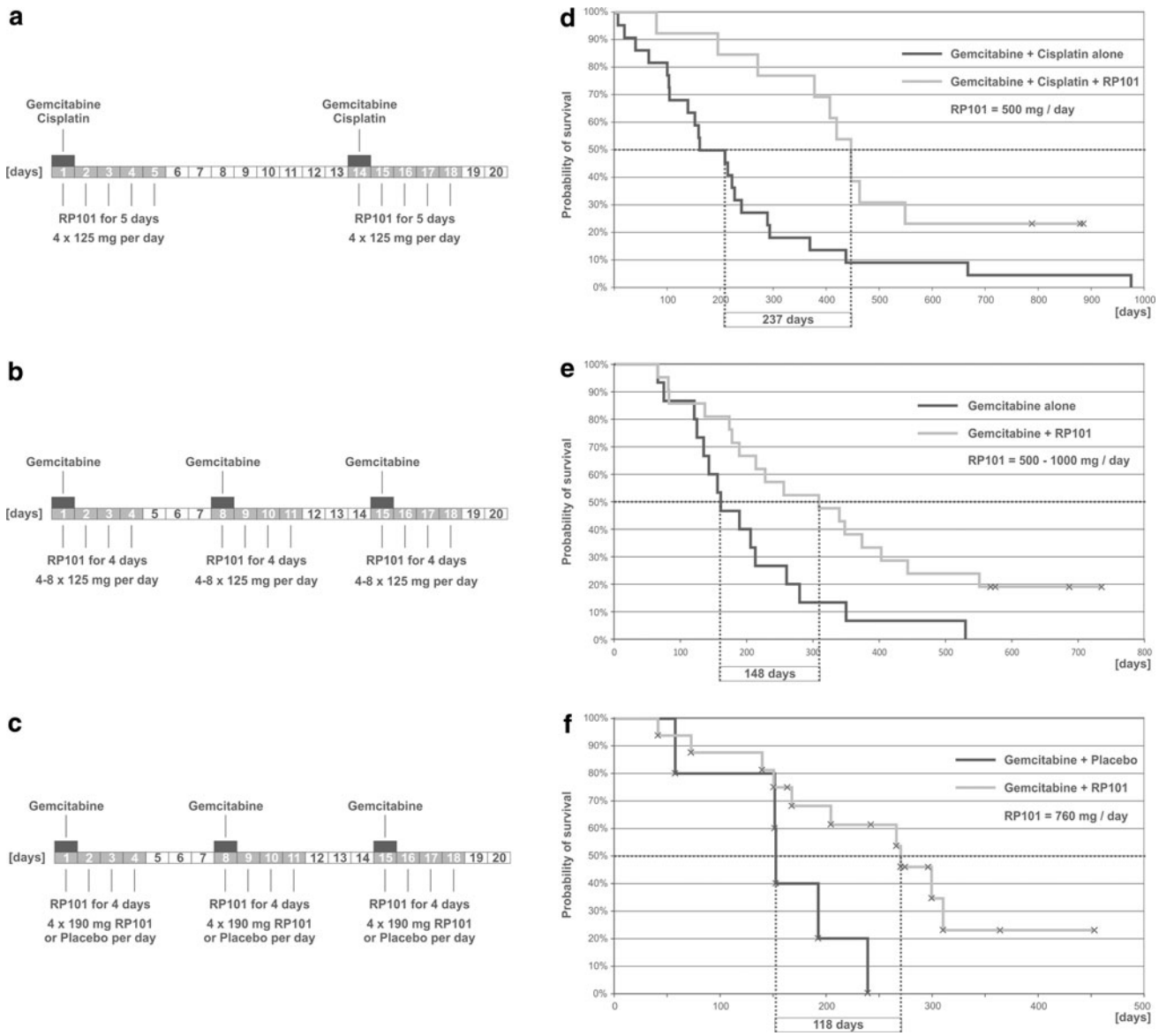

Fig. 5 RP101 co-treatment in clinical studies. **a** Two cycles of GEM + CIS + RP101 followed by 4 days RP101 "recovery" treatment in the pilot study. **b** Three cycles of GEM + RP101 followed by 3 days RP101 "recovery" treatment in the dose ranging study. **c** Three cycles of GEM + RP101 followed by 3 days RP101 "recovery" treatment in the phase 2 study: In this study, one tablet contains 190 mg RP101, per day four tablets were given to the patients. Kaplan–Meier survival curves of RP101 co-treatment in three different clinical trials. **d** Pilot study: RP101 + cisplatin + GEM. **e** Dose finding study: RP101 + GEM. **f** Phase II study: RP101 + GEM in heavy weight US-patients

This trend was also confirmed regarding the Severe Adverse Events (SAEs) grade 4 (life-threatening) and 5 (death related). In patients with a BSA $\leq 1.85\ m^2$, SAEs were lower in the GEM + placebo group (0.4 per patient) than in the GEM + RP101 group (0.7 per patient). The opposite effect was seen for patients with a BSA $\geq 1.85\ m^2$: 0.6 in the GEM + placebo group and 0.2 per patient in the GEM + RP101 group.

The total study population presenting with a BSA $\geq 1.85\ m^2$ showed a statistically significant positive trend (Cox regression, $P = 0.014$) regarding the beneficial effect of RP101 + GEM compared to patients with a BSA $< 1.85\ m^2$ (Fig. 6).

Subgroup US-patients

US-patients ($n = 40$) presented with an about 10 kg higher mean body weight and a higher BSA compared to patients from the rest of the world (ROW). While in ROW, only 50% of patients had a BSA $\geq 1.85\ m^2$; in the USA, this value equals 70%. In this study, the placebo + GEM US-patients showed a high but still realistic median survival of

Table 1 The influence of RP101 on Gemcitabine (GEM) levels (pharmacokinetic results)

A

Pharmacokinetic results of the influence of RP101 on the GEM levels

RP101 dose	RP101 ng/ml plasma conc.	RP101 half-life (h)	GEM ng/ml plasma conc.	GEM half-life (h)
125 mg	290 ± 152	1.980 ± 1.015	4.891 ± 1.532	0.275
	(n = 4)	(n = 2)	(n = 4)	(n = 1)
250 mg	1.549 ± 1.058	1.77 ± 1.14	13.254 ± 7.604	1.554 ± 2.4501
	(n = 17)	(n = 9)	(n = 17)	(n = 12)

B

Median survival phase 2 study

Patients	Median survival (months)			Significance
	GEM + placebo	GEM + RP101	Survival benefit of RP101 co-treatment	Log-rank
All 151 MITT[a] patients	8.87	6.70	−2.17	P = 0.0385
Patients BSA ≤ 1.85	8.87	6.60	−2.27	P = 0.0023
Trend MITT[a] patients				
Patients BSA ≥ 1.50 m²	9.46	6.80	−2.66	–
Patients BSA ≥ 1.75 m²	8.87	7.03	−1.84	–
Threshold BSA ≥ 1.85	6.41	6.90	+0.49	–
Patients BSA ≥ 1.95 m²	6.31	7.89	+1.56	–
Patients BSA ≥ 2.15 m²	5.73	9.96	+4.23	–
US-patients				–
All 40 US-patients	7.20	9.00	+1.80	–
US-patients BSA ≤ 1.85	8.87	8.90	+0.03	–
US-patients BSA ≥ 1.85	5.06	9.00	+3.94	P = 0.037

Median Survival in the Phase 2 study

[a] Modified intent to treat

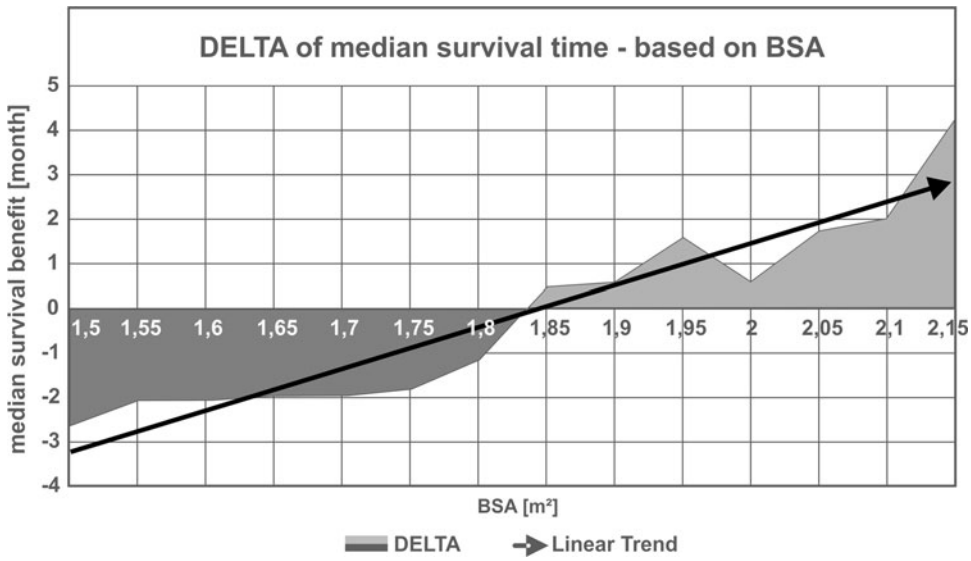

Fig. 6 Trend analysis. The chart shows the respective differences in median survival between the RP101- and the placebo group. Each value on the *horizontal axis* presents a BSA sub-group

7.20 months. The RP101 + GEM US-patients showed a median survival of 9.00 months, i.e., a benefit of 1.8 months. With respect to severe adverse side effects, there was no difference related to the higher body weight (0.5 vs. 0.45). Analyzing US-patients with a BSA ≥ 1.85 m² depicted a therapeutic benefit of RP101 + GEM with statistical significance (Table 1B; Fig. 5f).

Discussion

HSPB1 is expressed in many cancers and is known to control resistance against treatment with cytotoxic drugs, development of metastases, and prevention of apoptosis (Schmitt et al. 2007). It is expressed in response to a wide variety of physiological and environmental conditions including anticancer chemotherapy, allowing tumor cells to survive lethal conditions. Several effects are thought to account for the cytoprotective effect of HSPB1 (Garrido et al. 2006). The large number of negative effects on cancer progression and chemoresistance have led to HSPB1 becoming a novel target in cancer biology and its inhibition a new strategy in the development of innovative therapeutics (Arrigo et al. 2007). Several cancer cells overexpress HSPB1, and RP101 appears to down-regulate HSPB1 functions back to normal levels.

In previous work, we described RP101-effects that are related to HSPB1 as for example anti-recombinogenicity (Fahrig 1996), prevention of *mdr*1 gene amplification (Fahrig et al. 2000), enhancement of apoptosis (Fahrig et al. 2003), and prolonged survival of pancreas cancer patients (Fahrig et al. 2006). Now we show through magnetic pull-down experiments that HSPB1 was the target of RP101, and with an in silico structural model, we predicted the RP101 binding site. Mutation of the two key residues Phe29 and Phe33 in the predicted binding pocket prevented RP101 binding. The binding of RP101 to HSPB1 had important functional consequences: interaction with Pro-CASP3, AKT1, and CYC1 was inhibited. HSPB1 acts as a switch between apoptosis and survival by modulating AKT1 stability (Kanagasabai et al. 2010). Moreover, RP101 sensitized to heat shock and reduced tumor invasion in vitro. Its apoptotic effects were exemplified by the up-regulation of activated CASP9.

The results of our animal experiments showed that RP101 was only effective when given as co-treatment with a cytotoxic drug, and more precisely when given as single agent for some days following combination chemotherapy during the "recovery" phase. The treatment schedule of the three clinical studies performed, reflected these findings (see Fig. 5). In all three studies, RP101 has shown its potential to improve the survival of pancreatic cancer patients.

In the phase 2 study, the median survival was 8.87 months in the GEM plus placebo group and 6.70 months in the GEM plus RP101 group. Such a long survival for GEM only treated patients has never been observed before. In all other studies, the mean survival was 6 months, and in only two of 21 clinical studies, it was 7.2 months (Di Marco et al. 2010). Independent of the reasons for the long survival in the placebo plus GEM group and the impossibility to find out the reasons in retrospect, we focused our analysis on one observation of the dose finding study that higher dosage of RP101 could lead to an enhancement of GEM side effects. Therefore, we focused on the hypothesis that RP101 had been overdosed in the phase 2 study. It was hypothesized that heavyweight patients may have profited from co-treatment with RP101, but lighter patients might have suffered. The results confirmed the hypothesis: RP101 co-treated patients with a lower BSA than 1.85 had about twice as many SAEs grade 4 and 5 as patients treated with GEM alone. RP101 co-treated patients with a higher BSA than 1.85 had about one third of the SAEs grade 4 and 5 compared to patients treated with GEM alone. Following this train of thought, patients (and these are nearly exclusively men) with a BSA higher than 1.85 should profit from RP101 co-treatment. In accordance to this, the total study population presenting with a BSA higher than 1.85 showed a statistically significant positive trend regarding the beneficial effect of RP101 + GEM compared to patients with a BSA < 1.85 (Figs. 5f, 6). Patients treated with GEM only and with high BSA had a reduced life expectancy compared to patients with low BSA, whereas patients with high BSA co-treated with RP101 seem to profit and showed an increased survival. The beneficial effect of RP101 seen in the reduction in SAEs was reflected by an increase in median survival.

A statistically significant improvement of survival with RP101 co-treatment was observed only in US-patients with a BSA higher than 1.85 (Fig. 5f). This could be due to the fact that US-placebo + GEM patients showed a high but more realistic median survival of 7.2 months. Moreover, they had higher BSA compared to ROW-patients.

The dose of the pilot study (500 mg/day) had been chosen by considering doses used in animal experiments and by considering the experience gained in clinical studies where RP101 had been used as a virostatic drug. It was determined that doubling the dose of RP101 caused a disproportional fivefold increase in the concentration in the plasma, but the half-life of RP101 was not influenced. More importantly, the increase in GEM was about threefold, and the increase in the GEM half-life was 5.6-fold. These two effects together could be the explanation for the adverse events observed in the highest two doses (875 and 1,000 mg/day). The dose of 750 mg/day had been considered as being safe, but it was apparent that above a certain threshold of RP101, GEM-related side effects could appear. The increase in SAEs seen at higher concentrations of RP101 in lightweight patients is solely dependent on the plasma concentration and increase in GEM half-life, whereas the efficacy of RP101 is dependent on its binding to HSPB1. The patients of the following pivotal clinical study will be treated BSA-dependent.

Acknowledgments We thank C. Tuthill for the permission to publish the data of the SciClone phase 2 study, Th. Keller for the statistical analysis of BSA dependence, and C. Laverty for reviewing the manuscript.

Conflict of interest We declare that we have no conflict of interest.

References

Alexakis N, Halloran C, Raraty M, Ghaneh P, Sutton R, Neoptolemos JP (2004) Current standards of surgery for pancreatic cancer. Br J Surg 91(11):1410–1427

Arrigo AP, Simon S, Gibert B, Kretz-Remy C, Nivon M, Czekalla A, Guillet D, Moulin M, Diaz-Latoud C, Vicart P (2007) Hsp27 (HspB1) and alphaB-crystallin (HspB5) as therapeutic targets. FEBS Lett 581(19):3665–3674

Batchelder AJ, Gordon-Weeks AN, Walker RA (2009) Altered expression of anti-apoptotic proteins in non-involved tissue from cancer-containing breasts. Breast Cancer Res Treat 114(1):63–69

Bird LE, Ren J, Wright A, Leslie KD, Degreve B, Balzarini J, Stammers DK (2003) Crystal structure of varicella zoster virus thymidine kinase. J Biol Chem 278(27):24680–24687

Caillat C, Topalis D, Agrofoglio LA, Pochet S, Balzarini J, Deville-Bonne D, Meyer P (2008) Crystal structure of poxvirus thymidylate kinase: an unexpected dimerization has implications for antiviral therapy. Proc Natl Acad Sci USA 105(44):16900–16905

Champness JN, Bennett MS, Wien F, Visse R, Summers WC, Herdewijn P, de Clerq E, Ostrowski T, Jarvest RL, Sanderson MR (1998) Exploring the active site of herpes simplex virus type-1 thymidine kinase by X-ray crystallography of complexes with aciclovir and other ligands. Proteins 32(3):350–361

Chauhan D, Li G, Hideshima T, Podar K, Mitsiades C, Mitsiades N, Catley L, Tai YT, Hayashi T, Shringarpure R, Burger R, Munshi N, Ohtake Y, Saxena S, Anderson KC (2003) Hsp27 inhibits release of mitochondrial protein Smac in multiple myeloma cells and confers dexamethasone resistance. Blood 102(9):3379–3386

Di Marco M, Di Cicilia R, Macchini M, Nobili E, Vecchiarelli S, Brandi G, Biasco G (2010) Metastatic pancreatic cancer: is gemcitabine still the best standard treatment? (review). Oncol Rep 23(5):1183–1192

Fahrig R (1996) Anti-recombinogenic and convertible co-mutagenic effects of (E)-5-(2-bromovinyl)-2′-deoxyuridine (BVDU) and other 5-substituted pyrimidine nucleoside analogs in *S. cerevisiae* MP1. Mutat Res 372(1):133–139

Fahrig R, Steinkamp-Zucht A, Schaefer A (2000) Prevention of adriamycin-induced mdr1 gene amplification and expression in mouse leukemia cells by simultaneous treatment with the anti-recombinogen bromovinyldeoxyuridine. Anticancer Drug Des 15(5):307–312

Fahrig R, Heinrich JC, Nickel B, Wilfert F, Leisser C, Krupitza G, Praha C, Sonntag D, Fiedler B, Scherthan H, Ernst H (2003) Inhibition of induced chemoresistance by cotreatment with (E)-5-(2-bromovinyl)-2′-deoxyuridine (RP101). Cancer Res 63(18): 5745–5753

Fahrig R, Quietzsch D, Heinrich JC, Heinemann V, Boeck S, Schmid RM, Praha C, Liebert A, Sonntag D, Krupitza G, Hanel M (2006) RP101 improves the efficacy of chemotherapy in pancreas carcinoma cell lines and pancreatic cancer patients. Anticancer Drugs 17(9):1045–1056

Feng JT, Liu YK, Song HY, Dai Z, Qin LX, Almofti MR, Fang CY, Lu HJ, Yang PY, Tang ZY (2005) Heat-shock protein 27: a potential biomarker for hepatocellular carcinoma identified by serum proteome analysis. Proteomics 5(17):4581–4588

Garrido C, Brunet M, Didelot C, Zermati Y, Schmitt E, Kroemer G (2006) Heat shock proteins 27 and 70: anti-apoptotic proteins with tumorigenic properties. Cell Cycle 5(22):2592–2601

Hansen RK, Parra I, Lemieux P, Oesterreich S, Hilsenbeck SG, Fuqua SA (1999) Hsp27 overexpression inhibits doxorubicin-induced apoptosis in human breast cancer cells. Breast Cancer Res Treat 56(2):187–196

Harris AL, Hochhauser D (1992) Mechanisms of multidrug resistance in cancer treatment. Acta Oncol 31(2):205–213

Horton RM, Hunt HD, Ho SN, Pullen JK, Pease LR (1989) Engineering hybrid genes without the use of restriction enzymes: gene splicing by overlap extension. Gene 77(1):61–68

Hsieh M, Tsai HF, Chang WH (2005) HSP27 and cell death in spinocerebellar ataxia type 3. Cerebellum 4(1):31–36

Huang B, Schroeder M (2006) LIGSITEcsc: predicting ligand binding sites using the Connolly surface and degree of conservation. BMC Struct Biol 6:19

Jaattela M, Wissing D (1993) Heat-shock proteins protect cells from monocyte cytotoxicity: possible mechanism of self-protection. J Exp Med 177(1):231–236

Jemal A, Siegel R, Ward E, Murray T, Xu J, Thun MJ (2007) Cancer statistics, 2007. CA Cancer J Clin 57(1):43–66

Kamada M, So A, Muramaki M, Rocchi P, Beraldi E, Gleave M (2007) Hsp27 knockdown using nucleotide-based therapies inhibit tumor growth and enhance chemotherapy in human bladder cancer cells. Mol Cancer Ther 6(1):299–308

Kanagasabai R, Karthikeyan K, Vedam K, Qien W, Zhu Q, Ilangovan G (2010) Hsp27 protects adenocarcinoma cells from UV-induced apoptosis by Akt and p21-dependent pathways of survival. Mol Cancer Res 8(10):1399–1412

Kang SH, Kang KW, Kim KH, Kwon B, Kim SK, Lee HY, Kong SY, Lee ES, Jang SG, Yoo BC (2008) Upregulated HSP27 in human breast cancer cells reduces herceptin susceptibility by increasing Her2 protein stability. BMC Cancer 8:286

Karplus K (2009) SAM-T08, HMM-based protein structure prediction. Nucleic Acids Res 37(Web Server issue):W492–W497

Kase S, Parikh JG, Rao NA (2009) Expression of heat shock protein 27 and alpha-crystallins in human retinoblastoma after chemoreduction. Br J Ophthalmol 93(4):541–544

Lee JW, Kwak HJ, Lee JJ, Kim YN, Park MJ, Jung SE, Hong SI, Lee JH, Lee JS (2008) HSP27 regulates cell adhesion and invasion via modulation of focal adhesion kinase and MMP-2 expression. Eur J Cell Biol 87(6):377–387

Mahvi DM, Carper SW, Storm FK, Teal SR, Sondel PM (1993) Overexpression of 27-kDa heat-shock protein in MCF-7 breast cancer cells: effects on lymphocyte-mediated killing by natural killer and gamma delta T cells. Cancer Immunol Immunother 37(3):181–186

Mendez F, Sandigursky M, Franklin WA, Kenny MK, Kureekattil R, Bases R (2000) Heat-shock proteins associated with base excision repair enzymes in HeLa cells. Radiat Res 153(2):186–195

Mori-Iwamoto S, Kuramitsu Y, Ryozawa S, Mikuria K, Fujimoto M, Maehara S, Maehara Y, Okita K, Nakamura K, Sakaida I (2007) Proteomics finding heat shock protein 27 as a biomarker for resistance of pancreatic cancer cells to gemcitabine. Int J Oncol 31(6):1345–1350

Murr MM, Sarr MG, Oishi AJ, van Heerden JA (1994) Pancreatic cancer. CA Cancer J Clin 44(5):304–318

Nadin SB, Vargas-Roig LM, Cuello-Carrion FD, Ciocca DR (2003) Deoxyribonucleic acid damage induced by doxorubicin in peripheral blood mononuclear cells: possible roles for the stress response and the deoxyribonucleic acid repair process. Cell Stress Chaperones 8(4):361–372

Neoptolemos JP, Stocken DD, Friess H, Bassi C, Dunn JA, Hickey H, Beger H, Fernandez-Cruz L, Dervenis C, Lacaine F, Falconi M, Pederzoli P, Pap A, Spooner D, Kerr DJ, Buchler MW (2004) A randomized trial of chemoradiotherapy and chemotherapy after resection of pancreatic cancer. N Engl J Med 350(12):1200–1210

Nitiss JL (2009) Targeting DNA topoisomerase II in cancer chemotherapy. Nat Rev Cancer 9(5):338–350

Pandey P, Farber R, Nakazawa A, Kumar S, Bharti A, Nalin C, Weichselbaum R, Kufe D, Kharbanda S (2000) Hsp27 functions as a negative regulator of cytochrome c-dependent activation of procaspase-3. Oncogene 19(16):1975–1981

Phillips JC, Braun R, Wang W, Gumbart J, Tajkhorshid E, Villa E, Chipot C, Skeel RD, Kale L, Schulten K (2005) Scalable molecular dynamics with NAMD. J Comput Chem 26(16):1781–1802

Rane MJ, Pan Y, Singh S, Powell DW, Wu R, Cummins T, Chen Q, McLeish KR, Klein JB (2003) Heat shock protein 27 controls apoptosis by regulating Akt activation. J Biol Chem 278(30):27828–27835

Rocchi P, Beraldi E, Ettinger S, Fazli L, Vessella RL, Nelson C, Gleave M (2005) Increased Hsp27 after androgen ablation facilitates androgen-independent progression in prostate cancer via signal transducers and activators of transcription 3-mediated suppression of apoptosis. Cancer Res 65(23):11083–11093

Rocchi P, Jugpal P, So A, Sinneman S, Ettinger S, Fazli L, Nelson C, Gleave M (2006) Small interference RNA targeting heat-shock protein 27 inhibits the growth of prostatic cell lines and induces apoptosis via caspase-3 activation in vitro. BJU Int 98(5):1082–1089

Schmitt E, Gehrmann M, Brunet M, Multhoff G, Garrido C (2007) Intracellular and extracellular functions of heat shock proteins: repercussions in cancer therapy. J Leukoc Biol 81(1):15–27

Song H, Ethier SP, Dziubinski ML, Lin J (2004) Stat3 modulates heat shock 27 kDa protein expression in breast epithelial cells. Biochem Biophys Res Commun 314(1):143–150

Wang A, Liu X, Sheng S, Ye H, Peng T, Shi F, Crowe DL, Zhou X (2009) Dysregulation of heat shock protein 27 expression in oral tongue squamous cell carcinoma. BMC Cancer 9:167

Wessel D, Flugge UI (1984) A method for the quantitative recovery of protein in dilute solution in the presence of detergents and lipids. Anal Biochem 138(1):141–143

Wolff RA, Chiao P, Lenzi R, Pisters PW, Lee JE, Janjan NA, Crane CH, Evans DB, Abbruzzese JL (2000) Current approaches and future strategies for pancreatic carcinoma. Invest New Drugs 18(1):43–56

Xia Y, Liu Y, Wan J, Wang M, Rocchi P, Qu F, Iovanna JL, Peng L (2009) Novel triazole ribonucleoside down-regulates heat shock protein 27 and induces potent anticancer activity on drug-resistant pancreatic cancer. J Med Chem 52(19):6083–6096

Zhao L, Liu L, Wang S, Zhang YF, Yu L, Ding YQ (2007) Differential proteomic analysis of human colorectal carcinoma cell lines metastasis-associated proteins. J Cancer Res Clin Oncol 133(10):771–782